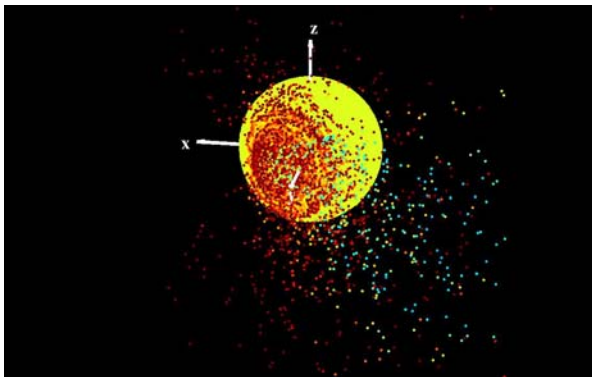


**CRUSTAL CONSEQUENCES OF PLANETARY-SCALE IMPACTS** Margarita M. Marinova<sup>1</sup>, Oded Aharonson<sup>1</sup>, and Erik Asphaug<sup>2</sup>, <sup>1</sup>Caltech, 150-21, Pasadena, CA 91125, mmm@caltech.edu, <sup>2</sup>University of California, Santa Cruz, Earth Sciences Dept., Santa Cruz, CA 95064

**Introduction:** Planetary-scale impacts, where the resulting crater cavity diameter is a significant fraction of the planet's circumference, are commonly observed in the Solar System: Caloris Basin on Mercury, South Pole-Aitken Basin on the Moon, Hellas Basin and possibly the Northern Lowlands on Mars, Herschel Crater on Mimas, and others. This size regime has not been extensively studied, yet the sphericity of the target and geometry of the gravity field are expected to significantly affect material redistribution, and thus also melt distribution. The change in crater properties with impact angle may be more prominent. For specificity, here we explore a large parameter space for planetary-scale impacts on early Mars, focusing on the resulting melt production and distribution, crustal excavation boundary size and ellipticity, crustal redistribution, depth of impactor penetration, antipodal disruption, escaping and orbiting material, and angular momentum transfer. Subsequent work will focus on impacts into other planetary bodies.

**Modeling:** We use a 3 dimensional Smoothed Particle Hydrodynamics (SPH) model to simulate the impacts (fig. 1). SPH is a Lagrangian method in which matter is represented by point masses smoothed over a particle radius. Pressure gradients and self-gravitating forces accelerate the particles; there is no material strength. SPH has been extensively used for simulating the Moon-forming impact [1]. In our simulations we nominally use 200,000 particles, giving a resolution (particle diameter) of  $\sim 118$  km; resolution effect studies show this to be sufficient to resolve the features of interest. The semi-empirical Tillotson Equation of State (EOS) is employed [2].



**Figure 1.** Simulation timestep ( $t = 0.58$  hrs) for a  $1.45 \times 10^{29}$  J, 10 km/s,  $45^\circ$  impact. Color represents internal energy

We simulate impacts with velocities of 6 to 50 km/s (5 km/s is Mars escape velocity, 50 km/s is twice

Mars orbital velocity), impact angles of  $0^\circ$  (perpendicular to planet surface),  $15^\circ$ ,  $30^\circ$ ,  $45^\circ$ ,  $60^\circ$ , and  $75^\circ$ , and impact energies of  $0.02 - 5.9 \times 10^{29}$  J (nominal 2,300 to 12,000 km craters; [3]).

To allow the accurate evaluation of melt production, a realistic planetary initial internal energy profile was developed. Surface and core-mantle boundary temperatures were set to those of parameterized convection models [4], and an adiabatic compression heating profile with depth was imposed to calculate mantle and core internal energies. The resulting pressure profile and core size are within the expected range [6, 7]. The bulk materials for the mantle and core are taken to be olivine and iron, respectively. An olivine ( $F_{075}$ ) EOS in the Tillotson formulation was developed [5]. A pressure-dependent forsterite melting criterion is used [8].

**Results:** The simulation results underscore the differences between small (well approximated by explosions in a half-space) and planetary-scale impact processes (where surface curvature and radial gravity are important).

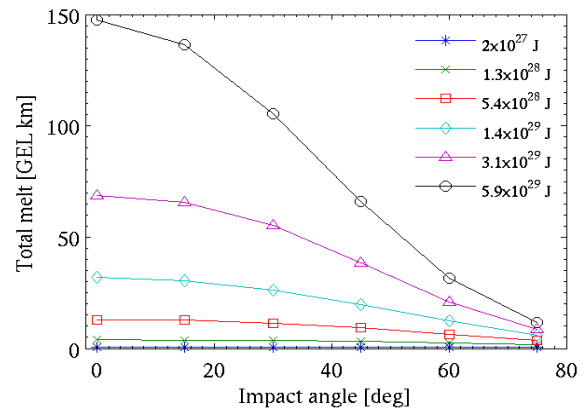


**Figure 2.** Melt production in terms of Global Equivalent Layer (GEL) depths; velocity averaged for each energy. 1 GEL km =  $5.1 \times 10^{20}$  kg.

We find that melt production chiefly scales with impact energy (approximately linearly) and impact angle (inversely), but is also affected by impact velocity. Despite the large representative melt GEL depths that result from the most energetic impacts (fig. 2), the distribution of melt on the surface is highly heterogeneous, with only  $\sim 30\%$  of the melt distributed on the surface outside of the crustal excavation boundary. Only for the highest energy, slow and low angle impacts, is more than half of the surface covered by melt, thus possibly resetting the surface and removing all evidence of the impact event.

The impacts are sufficiently energetic to penetrate into the mantle and excavate the overlying crust. The resulting crustal excavation boundary for a given impact energy is generally smaller than is predicted by small (half-space) crater scaling laws. For a given impact energy, increasing both impact velocity and angle significantly reduces the crustal excavation boundary. With increasing impact energy, the elongation resulting by an off-axis impact becomes apparent at smaller angles. For small craters, ellipticity is significant only for highly oblique impacts [9], highlighting the differences in the expression of small, half-space craters and planetary-scale impacts.

Planetary-scale impacts result in ejection distances comparable to the planetary circumference. This, together with the effect of surface curvature, results in the distribution of material over a larger surface area. We find that for impact energies  $> 10^{29}$  J and angles  $< 45^\circ$ , the ejecta does not lead to annular thickening around the excavation boundary. For highly oblique impacts ( $> 45^\circ$ ) as well as for lower impact energies, annular crustal thickening is present (fig. 3).

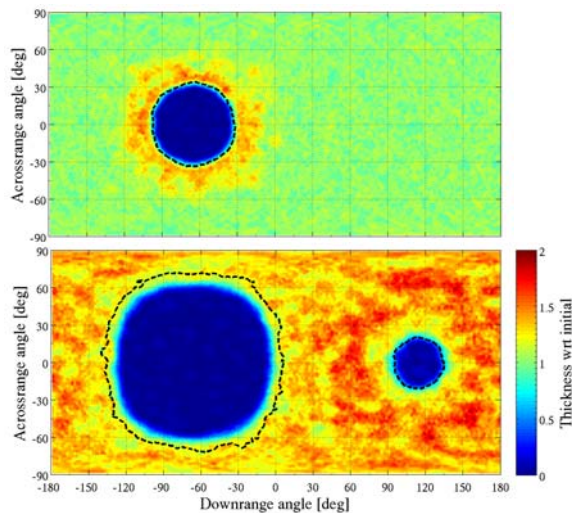


**Figure 3.** Crustal redistribution for low ( $5.4 \times 10^{28}$  J, top) and high ( $3.1 \times 10^{29}$  J, bottom) energy impacts. In both cases impact velocity is 10 km/s and angle is  $0^\circ$ . Antipodal disruption is present at the higher energy.

Penetration depth scales approximately linearly with momentum, as expected, and is modulated by impact angle. The highest momentum impacts reach the bottom of the mantle, however, no mixing with core material occurs. High amplitude planetary surface oscillations result from these energetic impacts, and may encourage volcanism due to a weakened lithosphere [10].

Antipodal disruption, including crustal removal and surface melting, is present for all energetic ( $> 10^{29}$  J), faster ( $> 6$  km/s), and less oblique impacts ( $\leq 45^\circ$ ).

In the parameter range investigated, the size of the antipodal disruption seen is up to  $70^\circ$  in diameter. For oblique impacts, the center of the disrupted zone is not antipodally aligned with the center of the crustal excavation boundary, with a maximum deviation of  $25^\circ$ .

All impact simulations result in orbiting material, down to the mass (particle) resolution. The highest ejected mass, for a given energy, is by slow (large), highly oblique impacts, yet the amount is only a fraction of the impactor's mass. However, impacts with velocities above  $\sim 20$  km/s are erosive, a result with relevance to accretion simulations.

The simulations show that planetary-scale impacts can contribute sufficient angular momentum to give a Mars-like planet a rotational period of order a day. The fastest rotation rates result from slow,  $\sim 45^\circ$  impacts. The size of impactors and impact velocities expected at the end of planetary accretion [11], as well as the most likely impact angle [12], are similar to the impact conditions shown by our simulations to produce an about 1 day rotational period on an initially stationary Mars.

The characterization of planetary-scale impacts is especially interesting with respect to understanding the impactors responsible for known impact structures, such as Hellas Basin (2000 km diameter). We have also applied our results to assess whether Mars' Northern Lowlands may be the result of a single large impact [3]. Our simulations show that a  $\sim 3 \times 10^{29}$  J (nominal 10,000 km crater) impact at 6 km/s and at a  $45^\circ$  angle produces features which are consistent with the Northern Lowlands characteristics [5].

The effects of differentiated impactors, as well as impacts into planets with smaller and larger relative core sizes than Mars are currently being investigated.

#### References:

- [1] Canup R.M. and Asphaug E. (2001) *Nature* 412, 708–712.
- [2] Tillotson J.H. (1962) General Atomic, San Diego, California, Report No. GA-3216, July 18.
- [3] Wilhelms D.E. and S.W. Squyres (1984) *Nature* 309, 138-140.
- [4] Hauck S.A. and Phillips R.J. (2002) *JGR* 107, 10.1029/2001JE001801.
- [5] Marinova M.M., Aharonson O., and Asphaug E. (2008) *Nature*, in press.
- [6] Bertka C.M. and Fei Y. (1998) *EPSL* 157, 79-88.
- [7] Yoder C.F. *et al.* (2003) *Science* 300, 299-303.
- [8] Asimow P.D. (2007) Goldschmidt Conference Abstracts.
- [9] Gault D.E. and Wedekind J.A. (1978) *EOS (Abstract)*59, 1121.
- [10] Elkins-Tanton L.T. and Hager B.H. (2005) *EPSL* 239, 219-232.
- [11] Hartmann W.K. and Davis D.R. (1975) *Icarus* 24, 504-515.
- [12] Shoemaker E.M. (1962) in *Physics and Astronomy of the Moon*. Academic Press.